

# Investigating the Simultaneous Process Design and Control of a Membrane Reactor for Hydrogen Production via Methane Steam Reforming

Alexios-Spyridon Kyriakides<sup>a</sup>, Panos Seferlis<sup>a,\*</sup>, Spyros Voutetakis<sup>b</sup>, Simira Papadopoulou<sup>c</sup>

<sup>a</sup>Department of Mechanical Engineering, Aristotle University of Thessaloniki, P.O. Box 484, 54124 Thessaloniki, Greece

<sup>b</sup>Chemical Process & Energy Resources Institute (C.P.E.R.I.), Centre for Research and Technology Hellas (CE.R.T.H.)  
 P.O. Box 60361, 57001, Thessaloniki, Greece

<sup>c</sup>Department of Automation Engineering, Alexander Technological Educational Institute of Thessaloniki, P.O. Box 141  
 57400 Thessaloniki, Greece  
[seferlis@auth.gr](mailto:seferlis@auth.gr)

In the present work, the simultaneous process design and control of a membrane reactor for H<sub>2</sub> production via methane steam reforming (MSR) is performed. The problem is stated as a non-linear optimization problem with non-linear constraints, which includes economic and controllability criteria in the objective function. A linear model predictive controller (MPC) is implemented to enforce the desired dynamic performance. Utilizing this methodology two pre-defined process flowsheets for H<sub>2</sub> production through the low temperature MSR, utilizing palladium-based membranes, are optimally designed based on economic criteria in the form of annualized capital and operating cost, and controllability criteria, in the form of the sum of squared errors during dynamic transitions. The first flowsheet is consisted of an integrated membrane reactor (IMR), whereas the second flowsheet under consideration is consisted of a cascaded arrangement between a reactor and a membrane module in series (CRM). Several other auxiliary processes such as heat exchangers, splitters, and mixers are employed. Rigorous nonlinear dynamic models have been developed assuming one dimensional transport and pseudo-homogenous conditions in the reaction zone in order to emulate the plant dynamics, whereas a linearized version of it is used by the MPC algorithm. Optimization results demonstrate the ability of the integrated process and control design framework to achieve a superior operating performance for a range of several factors affecting the operating conditions of the reactor.

## 1. Introduction

Increasing attention has been placed on the efficient hydrogen production with the utilization of carbon neutral feedstocks or renewable energy sources, as hydrogen is considered an ideal energy carrier and a key component of the future fuel market, due to its reduced greenhouse gas footprint (Čuček et al., 2015). The technological advances in clean energy production processes that utilize H<sub>2</sub>, such as fuel cells, has made the innovative design and development of H<sub>2</sub> production and purification systems an important aspect of sustainable process development research (Kravanja et al., 2015). A conventional method to produce H<sub>2</sub> from hydrocarbons fuels is MSR, where H<sub>2</sub> is separated from the reactor effluent synthesis gas. Additionally, significant emphasis has been placed on the study of process integration and design through the use of proper materials (e.g., catalyst), or equipment (membrane or fluidized bed reactor), aiming at making the process more efficient and economically attractive.

The intensification of processes has led to the development of processes that combine the step of production through MSR and the step of purification of H<sub>2</sub> through the utilization of palladium-based membranes into one IMR unit. The use of a membrane reactor, equipped with a Pd-based membrane that exhibits an extremely high selectivity towards H<sub>2</sub>, has proved to be a very promising choice. Hence, high CH<sub>4</sub> conversion can then be achieved at much lower reactor temperature than in conventional reactors (Kyriakides et al., 2014). The

intensified process results in a highly complex system where the interactions among the reforming reactions mechanism, the convective and molecular diffusion of the reacting mixture species, the diffusion of H<sub>2</sub> through the membrane, and the thermal effects due to reaction and heat exchange with an external heat source must be taken into consideration for the design of a highly performing system. The IMR system is influenced under real operating conditions by several factors that tend to deviate the process from the optimal operating point. A suitable control system aims to compensate for the effects of disturbances and maintain the production specifications. The design of such a control system is subject to limitations imposed primarily by the design decisions. In order to achieve the optimal economic performance, the process design and control design procedures should be conducted in an integrated fashion.

Although a significant number of studies deals with the definition of the optimal operating conditions and the optimal design of an IMR process, only a limited number of publications focus on the dynamic behaviour and on the design of a suitable control system. The optimal conditions (steam to carbon ratio, sweep gas flow rate) that minimize the overall CH<sub>4</sub> utilization along with the optimal reactor design configuration are presented by Kyriakides et al. (2016a). Murmura et al. (2017) presented a dimensionless analysis of the response of the reactor that focused on the pressure influence on the reactor product. The simultaneous maximization of CH<sub>4</sub> conversion, H<sub>2</sub> and CO selectivity has been reported by Shahhosseini et al. (2016), where a genetic algorithm was applied to derive the optimal Pareto front. The concept of auto-thermal membrane reformer is rigorously analysed by Patrascu and Sheintuch (2015). The minimum operating temperature for high thermal efficiency is defined, whereas a higher operating temperature is proposed in case of limited membrane area. Dynamic, one-dimensional, isothermal models for catalytic membrane reactor (Silva, 2014) and multi-scale, dynamic, two-dimensional, heterogeneous models for a traditional MSR reactor (Ghouse and Adams, 2013) have also been published. The design and implementation of an optimal MPC controller on an IMR was presented by Kyriakides et al. (2016b). A rigorous non-linear mathematical model was utilized to simulate reactor dynamics and the controller's ability to achieve the desired dynamic behaviour was confirmed. Wu et al. (2015) found the optimum operating conditions by maximizing the syngas yield subject to near-zero CO<sub>2</sub> emission constraints and verified the ability of a non-linear model-based control strategy to satisfy dynamic performance specifications.

The aim of this study is the development of integrated design framework for the optimal selection of process system design variables (unit operations and their interconnection, equipment capacities, operating conditions) utilizing a pre-defined control algorithm (MPC) of a membrane reactor for H<sub>2</sub> production under the presence of anticipated disturbances. The objective function incorporates the economic performance of the reactor system under steady state and dynamic conditions.

## 2. Mathematical model development

### 2.1 Integrated process design and control - optimization problem formulation

The problem of integrated process design and control is stated as a non-linear optimization problem, where a cost function including steady state and dynamic economic criteria along with dynamic performance metrics is minimized. A more general mathematical formulation of the problem can be depicted as a mixed-integer dynamic optimization problem. As shown in Eq(1), the cost function  $J$  depends on the differential, algebraic and control variables,  $(x(t), z(t), u(t))$ , the continuous process design variables and controller tuning variables,  $(d, d_c)$ , the integer variables associated with flowsheet configuration and control system input-output configuration,  $(X, X_c)$ , and on the uncertain parameters and disturbances,  $w(t)$ . The minimization problem is subject to the differential and algebraic equations of the process,  $(f, h)$ , the inequality constraints that define the feasible space,  $(g)$ , and on the controller problem statement expressed as an optimization problem with  $J_{MPC}$  the performance index subject to the differential and algebraic constraints  $(\varphi, \eta)$ .

$$\begin{aligned} & \text{Min}_{d, X, d_c, X_c} J(x(t), z(t), u(t), d, d_c, X, X_c, w(t)) \\ \text{st. : } & \begin{aligned} & f(\dot{x}(t), x(t), z(t), u(t), d, X, w(t)) = 0 \\ & h(x(t), z(t), u(t), d, X, w(t)) = 0 \\ & g(x(t), z(t), u(t), d, X, w(t)) \leq 0 \end{aligned} & \begin{aligned} & \text{Min}_{u(t)} J_{MPC}(\chi(t), \zeta(t), y(t), u(t), d_c, X_c) \\ & \text{s.t. } \varphi(\dot{\chi}(t), \chi(t), \zeta(t), y(t), u(t), d_c, X_c) = 0 \\ & \eta(\chi(t), \zeta(t), y(t), u(t), d_c, X_c) \leq 0 \end{aligned} \end{aligned} \quad (1)$$

### 2.2 Model predictive control

A multivariable model predictive control algorithm is considered in the integrated process design and control framework in order to calculate an optimal control action at each control interval. The control action satisfies a

performance index that includes the desired trajectory of controlled variable and the effort of the manipulated variables. A linearized process model requiring significantly less computational effort is employed for the process predictions with the overall control problem formulated as in Eq(2).

$$\min_{\Delta u} \left( \sum_{i=1}^{N_p} (y_{sp}(k+i) - y(k+i))^T Q (y_{sp}(k+i) - y(k+i)) + \sum_{i=1}^{N_c} \Delta u(k+i-1)^T R \Delta u(k+i-1) \right)$$

$$\text{s.t.:} \quad \begin{bmatrix} \overbrace{\Delta x_m(k+1)}^{x(k+1)} \\ y(k+1) \end{bmatrix} = \begin{bmatrix} A_m & 0_m \\ C_m A_m & 1 \end{bmatrix} \begin{bmatrix} \overbrace{\Delta x_m(k)}^{x(k)} \\ y(k) \end{bmatrix} + \begin{bmatrix} B_m \\ C_m B_m \end{bmatrix} \Delta u_m(k) \quad y(k) = \begin{bmatrix} c \\ 0_m & 1 \end{bmatrix} \begin{bmatrix} \overbrace{\Delta x_m(k)}^{x(k)} \\ y(k) \end{bmatrix} \quad (2)$$

$$\Delta u^{min} \leq \Delta u \leq \Delta u^{max} \quad u^{min} \leq u(k) \leq u^{max} \quad y^{min} \leq y(k) \leq y^{max}$$

where,  $y_{sp}$  is the output set-point,  $\Delta u$  the rate of change of the manipulated variables vector,  $y$  the controlled variables vector and  $x$  the augmented state variable vector.  $N_p$  and  $N_c$  are the lengths of the prediction and control horizon, and  $Q$  and  $R$  are properly adjusted weighting matrices. Also, the time (control) interval is set equal to  $T_s=30$  s. The MPC is formulated in the state space form, as described by Wang (2009), where the process system is described by a linear discrete time dynamic model. A more detailed description of the linear MPC algorithm utilized in the present work can be found in Kyriakides et al. (2016a).

### 2.3 Solution of the optimization problem

The mathematical formulation of the integrated process design and control framework described by the insertion of Eq(2) into Eq(1) is a non-linear dynamic optimization problem. The entire framework is developed and implemented in MATLAB software and is solved using the Simulated Annealing algorithm. At each iteration of the optimization algorithm, the steady-state part of the problem consisted a set of non-linear algebraic equations is solved together with the closed loop simulation. The controller uses a quadratic programming technique for the calculation of the optimal control actions at each interval in the simulation span.

## 3. Case study: Low Temperature Methane Steam Reforming

### 3.1 Flowsheet Configuration

The first flowsheet (IMR) considered is shown in Figure 1a. The configuration is mainly consisted of a reaction-separation module along with the heat exchanger modules required for the necessary heating of the reactants. More specifically, MSR process includes two reactants,  $\text{CH}_4$  which is pre-compressed and  $\text{H}_2\text{O}$  which is pressurized up to the reaction pressure.  $\text{H}_2\text{O}$  is directed to a steamer (HX-steam), while  $\text{CH}_4$  is heated in a heat exchanger (HX-methane). Steam flowrate is divided utilizing a splitter (SPLITTER) providing two streams, one heading to the mixer and another acting as the sweep gas in the IMR. Subsequently,  $\text{H}_2\text{O}$  and  $\text{CH}_4$  are fed into a mixer (MIXER) providing a stream containing the reactive mixture at a predefined molar S/C ratio. The reactive mixture is then fed to the membrane reactor (MR) where MSR and water-gas shift reactions take place over a Ni-based, foam supported (S-SiC with porosity of 85%) catalyst at a temperature range of 723 - 823 K and at reaction pressure of  $10^6$  Pa. A detailed description of the reaction scheme and kinetic model of the process can be found in Kyriakides et al. (2014), whereas a detailed description of the experimental unit based on which this reactor is modelled can be found in Kyriakides et al. (2016a). The reformer is a plug-flow reactor with external heating, where energy requirements are supplied by molten salts that exploit energy from solar troughs, enabling the minimization of the environmental impact of the process. The only constraint imposed by the use of molten salts is that the maximum operating temperature must be less than 823 K. Molten salt stream exiting the IMR module has sufficient enthalpy content so that it can be used at the steamer and heat exchanger in order to preheat the reactants. Membrane reactor's geometry is shown in Figure 1b. The reactor is consisted of three coaxial tubes, where the area inside the inner tube forms the permeation zone, the area between the inner and the middle tube forms the reaction zone, whereas the area between the middle and the outer tube forms the molten salts zone. The membrane (inner tube) is consisted of a 4-5  $\mu\text{m}$  Pd-based selective layer coated on a ceramic (porous  $\text{Al}_2\text{O}_3$ ) dense support. The difference between the square roots of  $\text{H}_2$  partial pressure in the reaction and in permeation zones is the driving force for  $\text{H}_2$  removal through the membrane. The second stream exiting the splitter is used as the sweep gas stream that flows through the permeation zone and carries the permeated  $\text{H}_2$  to storage, while maintaining higher driving force for  $\text{H}_2$  separation. Consequently, the permeate stream is fed to a condenser (HX-condenser) in order for the steam to be separated from  $\text{H}_2$ .

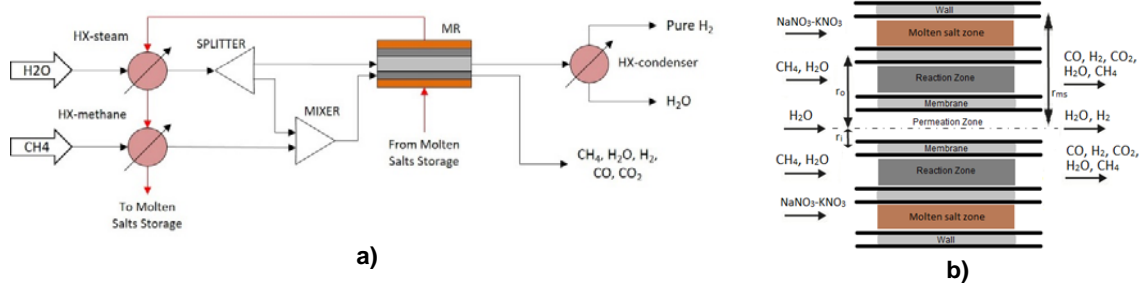


Figure 1: a) Integrated membrane reactor flowsheet (IMR) and b) reactor geometry configuration.

The second flowsheet (CRM) considered is shown in Figure 2. The configuration contains a reactor module, a membrane module and the necessary heat exchanger modules. After the heating of feed  $H_2O$  and  $CH_4$ , utilizing HX-steam and HX-methane heat exchanger units, steam is divided at splitter (SPLITTER) into two streams, one heading to the mixer and another used as the sweep gas in the separator. Subsequently,  $H_2O$  and  $CH_4$  are fed into a mixer (MIXER) which is then fed to the reactor (RE). IMR flowsheet's temperature, pressure and catalyst details also apply in this flowsheet. The stream exiting the reactor consists of a mixture at equilibrium composition and is fed to the separator (ME). Its geometry is similar to that of the membrane reactor, but limited to two coaxial tubes. The second stream exiting the splitter (SPLITTER) is consecutively used as a sweep gas in the separation module. Permeate from ME containing the sweep gas and the separated  $H_2$  are fed to a condenser (HX-condenser) in order for the steam to be separated from  $H_2$ . Molten salt stream exiting RE has enough energy left to fulfil the heating requirements at HX-steam and HX-methane.

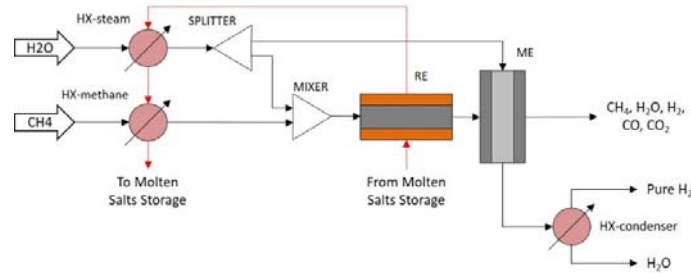


Figure 2: Cascaded reactor membrane flowsheet (CRM) configuration.

### 3.2 Membrane reactor, reactor and membrane separation modelling

Mathematical models, which describe the dynamic behaviour of the physicochemical phenomena occurring in the utilized modules are developed following Kyriakides et al. (2016). The dynamic, one-dimensional, nonlinear, pseudo-homogeneous mathematical model of the tubular membrane fixed-bed reactor is consisted of: a) mass balances for every component, Eq(3), b) energy balance, Eq(4), and c) momentum balance, Eq(5) in each zone. Parameter  $a$  is equal to 1 for reaction zone and 0 elsewhere, parameter  $b$  is equal to 1 when referring to  $H_2$  in reaction and permeation zone and 0 elsewhere and parameter  $c$  is equal to 1 in reaction and molten salt zone and 0 elsewhere. Similar models are employed in the CRM flowsheet.

$$\frac{\partial C_i}{\partial t} = -u \frac{\partial C_i}{\partial z} + a \rho_b \sum_{j=1}^3 R_j v_{i,j} - b \frac{2r_i}{r_o^2 - r_i^2} N_m, \quad i = CH_4, H_2O, H_2, CO, CO_2 \quad (3)$$

$$\rho C_p \frac{\partial T}{\partial t} = -u \rho C_p \frac{\partial T}{\partial z} + a \rho_b \sum_{j=1}^3 \Delta H r_j R_j + c \frac{2r_o}{r_o^2 - r_i^2} h_w (T_w - T) \quad (4)$$

$$\frac{\partial(\rho u)}{\partial t} + \frac{\partial(\rho u^2)}{\partial z} = 0 \quad (5)$$

Heat exchanger unit models employ simple energy balances for both cold and hot streams. Stream splitting modules utilize a mass balance, while maintaining the same concentration and temperature as the feed stream. Mixer modules employ mass and energy balances to compute the mass (flowrate and composition) and temperature of the exit stream.

### 3.3 Optimization within the integrated design and control framework

Given the process flowsheet configuration as well as the control algorithm with the set of manipulated variables, the mathematical formulation of the cost function can be simplified as in Eq(7), where the cost function and the process model and controller equations do not depend on controller tuning variables, ( $d_c$ ), and on the flowsheet configuration and control system input-output configuration, ( $X, X_c$ ). The cost function  $J$  is formulated in such way that it includes the sum of scaled design performance factors along with a controllability related index and is subject to the non-linear equations that describe the process dynamics and the linear equations that describe the controller.

$$\min_d \left( \frac{\sum_{i=1}^{N_{HE}} A_i}{A_{nom}} + \frac{\sum_{i=1}^{N_{Re}} \sum_{j=i,o,ms} R_{i,j}}{A_{nom}} + \frac{\sum_{i=1}^{N_{Re}} L_i}{A_{nom}} + \frac{F_{CH_4,in} + F_{H_2O,in}}{F_{nom}} + \left( \frac{pureH_2}{pureH_{2,nom}} - pureH_{2,target} \right)^2 + \int e^2 dt \right) \quad (7)$$

More specifically, the first three terms in Eq(7) represent the annualized capital cost, described by the dimensional characteristics of the process modules (namely the heat exchanger areas, reactor diameters and the length of the reactor). The fourth term represents the annualized operational cost that mainly depends on the CH<sub>4</sub> feed flowrate, whereas the fifth term represents the pre-defined pure H<sub>2</sub> production rate at steady state conditions. Finally, the ultimate term is the integral of squared errors for the controlled variables, which is used to assess the controller performance. Each term is multiplied by weight variables, properly chosen by the designer to reflect on their importance in the overall design objective function. Additional operational constraints, such as the range of steam to carbon ratio of the steam entering the reactor or temperature differences at heat exchanger modules, and decision variables bounds are enforced. During the dynamic simulation of the process, which is solved at every iteration of the optimization procedure, a set point change in the H<sub>2</sub> production rate along with a disturbance scenario are imposed to the system simultaneously. The imposed set point trajectory is shown in Figure 3a (dashed line) and the disturbance scenario in Figure 3b. The later involves a series of step changes in the pre-exponential factor of the Sieverts law that implies the deactivation of the Pd-based membrane, possibly due to competitive permeation.

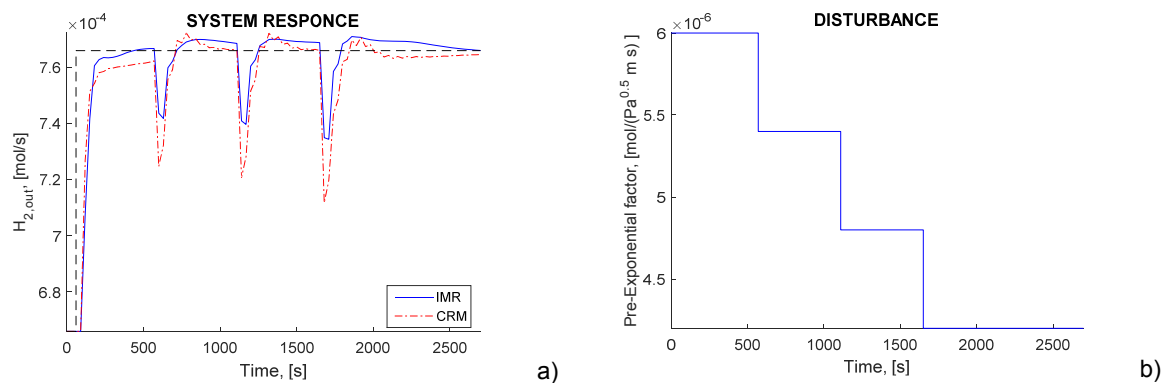


Figure 3: a) Pure H<sub>2</sub> production (controlled variable) for IMR (blue) and CRM (red) flowsheet and setpoint trajectory (black), b) Imposed disturbance scenario.

The dynamic behaviour of the closed loop simulation (Figure 3a) verify the controller's ability to cope with the tracking of the setpoints and the disturbance rejection in IMR and CRM flowsheets. Small deviations from the setpoint level occur at the time instances that the quite severe changes in the membrane permeability are imposed. The recovery of the production level is achieved with proper adjustment of CH<sub>4</sub> and H<sub>2</sub>O inlet flowrates and split ratio. Results referring to the decision variables obtained by the proposed methodology are reported in Table 1 indicating the different flowsheet configurations result in diverse design patterns. For instance, the thermodynamic limitations due to low operating temperature have a severe impact in CRM configuration. There is no membrane present inside the reactor and reaction cannot be shifted towards H<sub>2</sub> production. The CRM flowsheet configuration requires much larger (by a factor of 10) flowrates, in addition to a much larger reactor to produce the same pure H<sub>2</sub> amount as in the IMR flowsheet. The fact that in IMR flowsheet the reactive mixture is in direct contact with the membrane enables the simultaneous manipulation of the reaction and permeation zone conditions resulting in a better dynamic performance.

Table 1: Optimization results

Decision Variable	IMR flowsheet	CRM flowsheet
H <sub>2</sub> O inlet flowrate ( $F_{H_2O}$ , mol/s)	$8.72 \times 10^{-4}$	$3.59 \times 10^{-3}$
CH <sub>4</sub> inlet flowrate ( $F_{CH_4}$ , mol/s)	$1.81 \times 10^{-4}$	$1.15 \times 10^{-3}$
Splitter 1 ratio ( $a_1$ , -)	0.575	0.887
HX-steam heat exchange area ( $A_{ST}$ , m <sup>2</sup> )	0.0909	0.1776
HX-methane heat exchange area ( $A_{HEX}$ , m <sup>2</sup> )	0.3643	0.3170
HX-condenser heat exchange area ( $A_{CON}$ , m <sup>2</sup> )	0.4558	0.0527
Membrane reactor diameters ( $R_i$ , $R_o$ , $R_{ms}$ , m)	0.0097, 0.0436, 0.0837	-
Membrane reactor length (L, m)	0.9305	-
Reactor 1 diameters ( $R_i$ , $R_o$ , m)	-	0.0259, 0.0757
Reactor 1 length (L, m)	-	0.9784
Membrane 1 diameters ( $R_i$ , $R_o$ , m)	-	0.0105, 0.0864
Membrane 1 length (L, m)	-	0.3542

#### 4. Conclusions

A methodology for the integrated process design and control of two methane steam reforming flowsheets is performed. The objective function incorporates steady-state economic criteria and the dynamic performance of a model predictive controller in closed loop operation under the influence of disturbances and operational point transitions. The calculated design ensures the efficient operation and increased resilience under variation. The integrated reactor scheme exhibits superior performance than the cascaded system.

#### Acknowledgments

The research has received funding from the State Scholarship Foundation (IKY), especially under the framework of the program: "Fellowships of Excellence for Research Programs IKY/SIEMENS».

#### References

- Čuček L, Klemeš JJ, Varbanov PS, Kravanja Z, 2015, Significance of environmental footprints for evaluating sustainability and security of development. *Clean Technol. Environ. Policy*, 17(8): 2125-2141.
- Ghouse J.H., Adams T.A., 2013, A multi-scale dynamic two-dimensional heterogeneous model for catalytic steam methane reforming reactors. *Int. J. Hydrogen Energy*, 38(24), 9984-9999.
- Kravanja Z, Varbanov PS, Klemeš JJ, 2015, Recent advances in green energy and product productions, environmentally friendly, healthier and safer technologies and processes, CO<sub>2</sub> capturing, storage and recycling, and sustainability assessment in decision-making. *Clean Technol. Environ. Policy*, 17(5): 1119-1126.
- Kyriakides AS, Voutetakis S, Papadopoulou S, Seferlis P, 2016a, Optimization of an experimental membrane reactor for low temperature methane steam reforming, *Clean Technol. Environ. Policy*, 39(9), 1-11.
- Kyriakides AS, Seferlis P, Voutetakis S, Papadopoulou S., 2016b, Model Predictive Control for Hydrogen Production in a Membrane Methane Steam Reforming Reactor, *Chemical Engineering Transactions*, 52, 991-996.
- Kyriakides AS, Rodriguez-Garcia L, Voutetakis S, Ipsakis D, Seferlis P, Papadopoulou S, 2014, Enhancement of pure hydrogen production through the use of membrane reactor, *Int. J. Hydrogen Energy*, 39(9), 4749-4760.
- Murmura MA, Cerbeli S, Annesini MC, 2017, Transport-reaction-permeation regimes in catalytic membrane reactors for hydrogen production. The steam reforming of methane as a case study, *Chemical Engineering Science*, 162, 88-103.
- Patrascu M, Sheintuch M, 2015, Design concept of scaled-down autothermal membrane reformer for on board hydrogen production, *Chemical Engineering Journal*, 282, 123-136.
- Shahhosseini HR, Farsi M, Eini S, 2016, Multi-objective optimization of industrial membrane SMR to produce syngas for Fischer-Tropsch production using NSGA-II and decision makings, *J. Nat. Gas Sci. Eng.*, 32, 222-238.
- Silva JD, 2014, Dynamic Simulation of the Steam Reforming of Methane for the Production of Hydrogen in a Catalytic Fixed Bed Membrane Reactor, *Chemical Engineering Transactions*, 39, 961-966.
- Wang L, 2009, *Model Predictive Control System Design and Implementation Using MATLAB*. Springer, London, England.
- Wu W., Yang H.T., Hwang J.J., 2015, Dynamic control of a stand-alone syngas production system with near-zero CO<sub>2</sub> emissions, *Energy Convers. Manage.*, 89, 24-33.